Quantum-Mechanical Study of Thermodynamic and Bonding Properties of MgF_2

E. Francisco,* J. M. Recio, M. A. Blanco, A. Martín Pendás, and A. Costales

Departamento de Química Física y Analítica, Facultad de Química, Universidad de Oviedo, 33006-Oviedo, Spain

Received: August 1, 1997; In Final Form: October 15, 1997

The structural and thermodynamic properties of MgF_2 have been investigated in a wide range of pressures (0−80 GPa) and temperatures (0−850 K) by coupling quantum-mechanical ab initio perturbed ion calculations with a quasi-harmonic Debye model. The room temperature, zero-pressure structural parameters and lattice energy are computed with errors smaller than 2% when correlation energy corrections are incorporated in the calculation. Our computed equation of state is compatible with direct measurements of the bulk modulus and obeys universal $p-V$ relations. We have simulated the rutile-to-fluorite phase transition during the loading process and have found lower (≃4 GPa) and upper (≃45 GPa) bounds for the transition pressure by means of thermodynamic and mechanical criteria for phase stability. Bonding properties and their change with pressure have been derived through a topological analysis of the electron density using Bader's theory of atoms in molecules. This analysis reveals that MgF_2 is a highly ionic compound. Its ionicity decreases linearly with increasing pressure and, as in other ionic compounds, the crystal shows anion−anion bonds.

I. Introduction

Although the observable properties of MgF_2 have been experimentally explored over the years,[1−13] theoretical simulations on this crystal have been scarce and usually limited to fixed values of pressure (p) and/or temperature (T). Early simulations based on interionic potentials were concerned with cohesive, static properties ($T = 0$, and zero-point vibrational effects neglected) at $p = 0$.[14,15] Recently, Kim, and Choo[16] minimized the total energy in the rutile phase at static conditions and calculated harmonic−lattice dynamical properties at the optimized geometry using empirical potentials. As these authors point out, such work should be extended to analyze the anharmonicity effects on the structural and dynamical properties and to explore the pressure-induced rutile to fluorite phase transition. This transition has been recently studied at a fixed T in terms of empirical potentials using lattice dynamics[17] and molecular dynamics[18] techniques. These two approaches give very different values for the transition pressure.

Crystal simulations have also been reported from pure quantum-mechanical methods, the more detailed study of this sort being that of Catti et al.[19] They have computed structural parameters and elastic constants of MgF_2 with the Hartree−Fock (HF) method implemented in the program CRYSTAL. Their calculations, in the static, zero-pressure approximation, partially optimize the geometrical parameters of the rutile phase and include correlation energy corrections at the final stage.

The study of these works suggests the necessity of extending the theoretical analysis of the structural stability, equation of state, and electron density of this important material.

We present in this paper the results of an investigation on these three questions. Our approach is totally nonempirical and combines HF plus electron correlation calculations of the electronic structure, the determination of the equation of state and other thermodynamic properties in a wide range of pressure and temperatures, and a rigorous analysis of the electron density. The necessary theoretical tools to undertake this approach include: (a) static ab initio perturbed ion (*ai*PI) calculations, with correlation energy corrections,[20,21] to optimize the structural parameters of MgF_2 from $p = 0$ GPa to $p = 80$ GPa; (b) a quasi-harmonic Debye model, based on the quantum-mechanical energy−volume function, to compute the vibrational contributions to the thermodynamic properties of this crystal; and (c) a topological analysis of the crystal electron density using Bader's *Atoms in Molecules* theory,[22] as adapted by our group to the study of periodic systems.[23,24] From this analysis we compute ionic shapes, volumes, and charges, as well as their change with pressure.

We examine in detail the advantages and limitations of this nonempirical approach by discussing its performance in the determination of a variety of structural, thermodynamic, and bonding properties of this material. We show that a crystal with three structural degrees of freedom can be analyzed from first principles in a way that permits the interpretation of thermodynamic experimental information obtained from different sources. The equation of state at finite T can be computed in agreement with (p,V,T) data and direct observations of the bulk modulus. The variation of the crystal ionicity with applied pressure can be predicted from the analysis of the electronic density. We also see that the quantum-mechanical method adopted here needs further improvements to accurately deal with nonspherical ionic charge distributions and crystal polarization.

The simulation techniques are described in subsections II.A, B, and C. Results for the static structural and thermodynamic properties at zero pressure are discussed in subsection III.A. Subsections III.B and III.C are dedicated to analyze the equation of state and the pressure-induced rutile-to-fluorite phase transition, respectively. The main findings concerning the topological atomic properties are presented in subsection III.D. We summarize our conclusions in section IV.

II. Simulation Techniques

A. Total Energy Calculations and Geometry Optimizations. MgF_2 crystallizes in the rutile phase at ambient conditions. This structure belongs to the tetragonal space group

S1089-5639(97)02516-4 CCC: $15.00
Published on Web 02/07/1998

$P4_2/mmm$ with two molecules in the unit cell. The positions of the two Mg atoms are fixed at the symmetry sites (0,0,0) and ($^1/_2$,$^1/_2$,$^1/_2$), and the four F atoms are placed at (u,u,0), ($-u$,$-u$,0),($^1/_2-u$,$^1/_2+u$,$^1/_2$), and ($^1/_2+u$,$^1/_2-u$,$^1/_2$), u being a fractional coordinate. This space group is characterized by three geometrical parameters: the two unit cell lengths (a,c) and the internal coordinate u. From now on, we will refer collectively to the set [a,c,u] as $\vec{x}$.

Given a value of $\vec{x}$, we compute the total energy of the MgF_2 crystal by solving the localized Hartree−Fock (HF) equations implemented in the *ai*PI model.[20,21] As in previous calculations within this theoretical scheme,[25] we employ the nearly-HF, multi-ζ exponential basis sets of Clementi and Roetti,[26] and estimate the correlation energy through the unrelaxed Coulomb Hartree−Fock approximation (uCHF).[27]

As a first step, we perform a static simulation both at the HF and HF+uCHF levels. In these calculations, the Gibbs energy at a given pressure p ($G_{static}(\vec{x};p) = E_{latt}(\vec{x}) + pV(\vec{x})$) is minimized simultaneously with respect to the three geometrical parameters contained in $\vec{x}$ by means of a modified multidimensional Powell algorithm,[28] taking into account that the pV term does not depend on u. In the above expressions, $E_{latt}(\vec{x})$ is evaluated as the difference between the total energy per unit formula of the crystal and the energy of the isolated ions ($Mg^{2+} + 2\ F^-$).

Our procedure goes beyond previous quantum-mechanical zero-pressure computations in this crystal[19] in two important points: (i) effects of correlation energy corrections are included at each $\vec{x}$ point in the optimization process and not only at the HF optimized configuration and (ii) the minimization search is direct, three-dimensional, and does not use any experimental parameter. By repeating our optimization process for different p's we obtain the pressure dependence of $\vec{x}$ and the static equation of state (EOS) through the $V(\vec{x}) = {}^1/_2(a^2c)$ relation.

In a second step, we generate thermodynamic results at finite temperatures using a Debye-type model that is detailed in the next subsection. The input for this model is a set of (E_{latt},V) points which cover a volume range ∼−30% to ∼+50% of the static equilibrium volume at zero pressure, V_0. For volumes greater than V_0, we obtain (E_{latt},V) pairs by minimizing G_{static} with negative pressures.

B. Thermal Effects. We have chosen a Debye-like model to take into account the vibrational motion of the lattice. Our scheme, while retaining the simplicity of the original Debye model, follows a quasi-harmonic approach, making the Debye temperature Θ dependent upon the volume of the crystal. At every volume V, Θ(V) is rigorously defined in terms of the elastic constants through a spherical average of the three components of the sound velocity. The latter may be obtained by solving the Christoffel equations of the crystal.[29] Computationally, however, this procedure would imply the accurate calculation of all the independent elastic constants of the crystals at every pressure of interest. This is a highly demanding task, and has been simplified through the isotropic approximation, which allows to evaluate Θ using the expression[30]

$$\Theta = \frac{\hbar}{k_B}[6\pi^2 V^{1/2} r]^{1/3}\sqrt{\frac{B_S}{M}}\, f(\sigma) \qquad (1)$$

where $\hbar$ is the reduced Planck constant, k_B is the Boltzmann constant, M the molecular mass of the compound, r the number of atoms per molecular unit ($r = 3$ in the case of MgF_2 crystal), B_S the adiabatic bulk modulus of the crystal, and σ the Poisson ratio.[30] This property is crystal dependent and changes slightly with T and p. In order to avoid the σ-dependence of Θ, we set $\sigma = 0.25$, the value of the Cauchy solid.[30] This value is close to that obtained by Kandill et al.[31] from room temperature ultrasonic experiments on single crystals ($\sigma = 0.271$).

The explicit expression for $f(\sigma)$ in eq 1 is[30]

$$f(\sigma) = \left\{3\left[2\left(\frac{2}{3}\frac{1+\sigma}{1-2\sigma}\right)^{3/2} + \left(\frac{1}{3}\frac{1+\sigma}{1-\sigma}\right)^{3/2}\right]^{-1}\right\}^{1/3} \qquad (2)$$

This function decreases almost linearly with σ in the vicinity of $\sigma = 0.25$ and it takes the value $f(\sigma = 0.25) = 0.859\ 95$, that should be compared with $f(\sigma = 0.271) = 0.818\ 26$. In the explored temperature range, the computed values of V_0 and B_0 (see below) change by less than 0.4% and 1.0%, respectively, in going from $\sigma = 0.2$ to $\sigma = 0.3$.

In eq 1, B_S depends on V and T. In order to balance computational demand and accuracy, we have introduced a further approximation that reduces Θ to a function of V:

$$B_S \simeq B_{static} = V\left(\frac{d^2E_{latt}(V)}{dV^2}\right) \qquad (3)$$

where B_{static} is the static bulk modulus. It is evident from eqs 1 and 3 that there is no explicit consideration of the geometrical parameters $\vec{x}$ in the volume derivatives, since we restrict ourselves to hydrostatic conditions. This relevant feature of the model makes it fully independent of any particular crystal structure. Even if the crystal energy depends on many internal parameters and cell constants, a set of pairs (E_{latt},V) is sufficient to run the model. The approach has its main drawback in the fact that the geometrical parameters are functions of the volume only. This is equivalent to assume that thermal dilatation changes the structural parameters of a crystal in the same way as a hydrostatic expansion does.

In order to obtain the equilibrium volume at constant p and T, we minimize the Gibbs function with respect to V. The *nonequilibrium G* is given by

$$G^*(V;T,p) = E_{latt}(V) + pV + F_{vib}(T,\Theta(V)) \qquad (4)$$

where F_{vib} is the vibrational Helmholtz function, including zero-point contributions, as given by the Debye model. The $V(T,p)$ curve or EOS is implicitly defined by the relation:

$$\left(\frac{dG^*(V;T,p)}{dV}\right) = 0 \qquad (5)$$

and the isothermal bulk modulus is given by

$$B_T(T,p) = V(T,p)\left(\frac{d^2G^*(V;T,p)}{dV^2}\right) \qquad (6)$$

In order to simplify the minimization and derivation processes involved in eqs 5 and 6, it is convenient to fit an appropriate analytical function of V to the numerically computed values of $G^*(V;T,p)$.[32] From this function, the Debye temperature at $V(T,p)$ and all the vibrational properties (U_{vib}, $C_{v,vib}$, F_{vib}, and S_{vib}) are immediately computed. Moreover, since our Debye temperature depends only on volume, the Mie−Grüneisen equation applies to our model, and the Grüneisen constant γ and other experimentally available properties such as the thermal expansivity (α), the adiabatic bulk modulus (B_S), and the isobaric heat capacity (C_p) may be readily obtained.

C. Bader Topological Analysis. Bader's theory of *Atoms in Molecules*[22] has probably provided the first sound foundation to the phenomenological models of chemical bonding. Briefly,

TABLE 1: Zero-Pressure Structural and Thermodynamic Equilibrium Properties of the MgF_2 Rutile Phase[a]

	a	*c*	*c*/*a*	*u*	E_{latt}	$S°(298.15)$	$H°(298.15) - H°(0)$
static (HF)	8.7817	5.9802	0.6810	0.3044	−2851		
static (HF+uCHF)	8.5262	5.8191	0.6825	0.3047	−3025		
0 K (HF+uCHF)	8.576	5.847	0.6818	0.3048	−3005		
300 K (HF+uCHF)	8.600	5.860	0.6813	0.3048	−2997	47.3	8.88
ref 19 (HF)	8.7626	5.8336	0.6657	0.3032			
ref 16	8.674	5.788	0.6673	0.3036			
experimental	8.721[b]	5.750[b]	0.6594[b]	0.3030[b]	−2957[c]	57.2 ± 0.5[c]	9.91 ± 0.06[c]
	8.733[d]	5.767[d]	0.6604[d]	0.30293[d]			

[a] Units for *a* and *c* are bohr, for E_{latt} and *H* are kJ/mol, and for *S* are J/(mol K). [b] $T = 50$ K. Reference 12. [c] Room temperature. Reference 33. [d] Room temperature. Reference 7.

the method originates in the fact that the laws of quantum mechanics hold in localized regions of space surrounded by surfaces whose flux of the gradient of the electron density vanishes. These topological regions are usually associated to one nucleus, so an unambiguous definition of an atom in a molecule appears. The method shows that integration of appropriate operators over those atomic regions gives rise to additive *atomic properties*. Moreover, different types of critical points of the electron density are associated to different bonding features. Objective answers to the question of when two atoms are bonded are so obtained.

We have recently investigated[23,24] the application of this theory to periodic crystalline systems. We simply recall here that finding the whole set of critical points of a crystalline structure is not an easy task. One of the main difficulties lies on the large number of critical points that must be obtained in a very small volume and in the low value of the electron density that may be found in some bonding regions, particularly in ionic crystals. Visualization of the actual atomic shapes makes it necessary to use computational geometry tools to fully understand the organization and relations among volumes in three-dimensional space. To face both problems, we have constructed an efficient code[23] for determining automatically topological properties of simple structures and producing source data to feed high-performance rendering programs. This technology has been used to analyze the topology of the electron density of MgF_2 in its rutile phase and to follow its change with pressure.

III. Results and Discussion

A. Zero-Pressure Structural and Thermodynamic Properties. First, we will briefly discuss the static properties of MgF_2, as a preliminary stage to the study of its thermal behavior. The static HF and HF+uCHF calculations produce two different sets of equilibrium values for $\vec{x}$ and E_{latt}. These results are collected in Table 1 with other calculated and experimental values. Our values are consistent with the expected effects of the correlation energy: a reduction of the cell constants and the crystal energy. Inclusion of the correlation energy correction lowers the molecular volume by some 9%, and the lattice energy by about 174 kJ/mol. The internal coordinate *u* and the *c*/*a* ratio are quite insensitive to this correction.

Our static HF lattice parameters are higher than those computed by Kim and Choo.[16] This result is normally observed when comparing HF results with those deduced from empirical potentials. The static *ai*PI results and those of Catti *et al.*[19] give lattice parameters larger than the values observed at room temperature. The HF+uCHF description corrects this deviation and it is an adequate starting stage for the inclusion of thermal effects. Moreover, as Figure 1 reveals, a quantitative agreement with the experimental $V(T)$ data can only be achieved when correlation corrections are included. Thus, we will concentrate in the HF+uCHF results in the rest of this subsection.

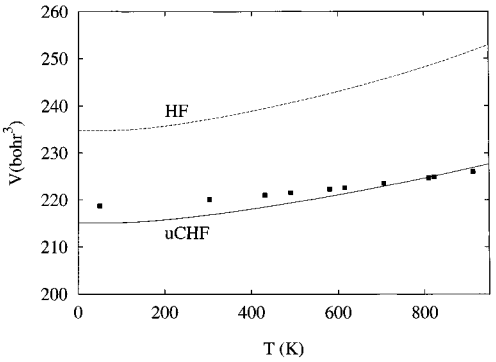

Figure 1. Zero-pressure temperature dependence of the unit cell volume for the MgF_2 rutile phase according to our HF and HF+uCHF calculations. Symbols stand for experimental data of ref 3, except the value at 50 K from ref 12.

In the Debye-like model used here, the second derivative of E_{latt} determines Θ as a function of *V*. We find $\Theta = 713$ K at the static equilibrium volume and $\Theta = 680$ K at 300 K. Following the exact procedure commented in subsection II.A, we have derived from the elastic data of Jones[10] an *experimental* room temperature value $\Theta_{exptal} = 614$ K.

The increase of *a*, *c*, and E_{latt} due to thermal effects leads to discrepancies smaller than 2% with the experimental structural parameters.[7] E_{latt} deviates 1.3% from the observed value of 2957 kJ/mol.[33] A comparison with the static results shows that two thirds of the thermal increase in the cell size is due to zero-point contributions. In E_{latt} the zero-point energy (20 kJ/mol) accounts for 71% of the difference between the static and the 300 K calculations. The computed normal entropy $S°(298.15)$ and enthalpy $H°(298.15) - H°(0)$ deviate 17% and 10% from the corresponding measured values.[33] All this information is collected in Table 1. In general terms, our results describe the zero-pressure MgF_2 rutile structure in rather good agreement with the observed behavior. This is a necessary status for extending the simulation to the study of the crystal response to external pressure.

A set of magnitudes that are specially sensitive to computational details are those related to the volume dependence of Θ, since they involve third derivatives of the static lattice energy. The most important factor in computing this set of properties is the Grüneisen constant γ. According to our calculations, $\gamma = 1.959$ at the equilibrium volume at 300 K. Using experimental data at room temperature, we have obtained $\gamma_{exptal} = 1.34$. This difference explains in part the discrepancy between our computed thermal expansivity $\alpha = 53.7 \times 10^{-6}$ K^{-1} and the experimental one[3] (32.4×10^{-6} K^{-1}). This result is illustrated in Figure 1 where, in spite of the good agreement between the observed and computed HF+uCHF $V(T)$ points, the difference in slopes is apparent.

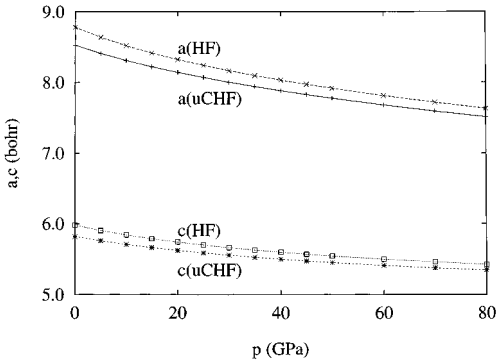

Figure 2. Pressure dependence of the unit cell lengths for the MgF_2 rutile phase according to our static HF and HF+uCHF calculations.

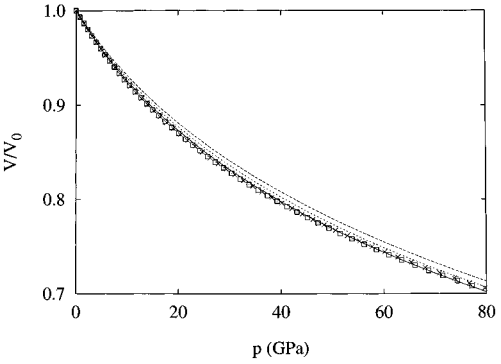

Figure 3. Static (dashed), $T = 0$ K (dotted), and $T = 300$ K (solid) equations of state for the MgF_2 rutile phase according to our HF+uCHF calculations. Squares and crosses stand for Birch-Murnaghan and Vinet empirical equations of state, respectively.

B. Equation of State. We start the study of pressure effects by analyzing the static results at the HF and HF+uCHF levels. The evolution of the unit cell lengths a and c with p is shown in Figure 2. As expected, the HF parameters are larger than the HF+uCHF ones in the whole range of pressures, the corresponding curves being nearly parallel for both parameters. The slopes da/dp and dc/dp at zero pressure are slightly smaller in the HF+uCHF stage. This result agrees with the expectation of a less compressible MgF_2 when correlation effects are included in the calculation. We observe in Figure 2 that a decreases with pressure more steeply than c, revealing an anisotropy under applied pressure. The c/a ratio turns out to be an increasing and almost linear function of p. This larger compressibility along the a direction agrees with the analysis of the experimental elastic constant data.[9] As in the zero-pressure stage, the correlation energy corrections do not change significantly the c/a HF ratios. For instance, at 100 GPa c/a(HF) = 0.7184 and c/a(HF+uCHF) = 0.7188. The temperature effect on the c/a ratio at zero p is almost negligible, in agreement with observations.[3] The u parameter varies slightly with external pressure. From 0 to 100 GPa, it ranges 0.3040−0.3060 (HF) and 0.3045−0.3065 (HF+uCHF). A slight dependence of the internal coordinates with thermodynamic variables is common in many crystals. Analysis of the data reported by Ming and Manghnani[11] gives $a = 8.50$ and $c = 5.37$ b at 25 GPa. Our computed values at this pressure ($a = 8.111$ and $c = 5.609$ b) deviate less than 5% from these experimental data.

To analyze the $V(p)$ behavior we use the $V(T,p)/V_0(T) = V/V_0$ *versus* p diagram (Figure 3). We find that the compressibility of MgF_2 increases with T and when the zero-point vibrational effects are taken into account. We include in Figure 3 the $V/V_0 - p$ points computed with the experimental athermal B_0 value of Jones[10] and $B_0' = 4.5$. The latter values were obtained assuming two different and well checked empirical EOS: the frequently used Birch−Murnaghan form and the more recent Vinet EOS (VEOS).[34] We find that these two functional forms yield almost coincident values along the explored $V(p)/V_0$ range. Also, our HF+uCHF calculations predict a pressure dependence of the V/V_0 ratio in very good agreement with both EOS.

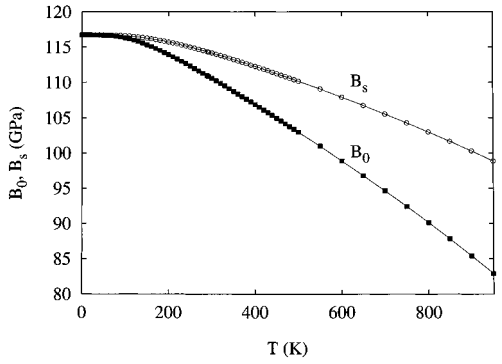

Figure 4. Temperature dependence of the isothermal (B_0) and adiabatic (B_S) zero-pressure bulk modulus of the MgF_2 rutile phase according to our HF+uCHF calculations.

Our computed values for the zero-pressure isothermal and adiabatic bulk moduli ($B_T(p = 0) = B_0$ and B_S) and their pressure and temperature derivatives are quantitatively compared with other theoretical[19] and experimental[8−10,13] data in Table 2. Once again, our HF static predictions agree with the calculated values from ref 19, being also close to the room temperature experimental data. The inclusion of correlation corrections and thermal effects give theoretical values deviating less than +7% from the experiment (see also Figure 3).

A comparison between the isothermal and adiabatic bulk moduli at zero pressure (B_0, B_S) allows us to investigate the different response of MgF_2 to the increase of pressure in isothermal or adiabatic conditions. The computed values of these two magnitudes in the HF+uCHF calculation are plotted versus T in Figure 4. B_0 and B_S are nearly constant from 0 to 100 K and decrease almost linearly with increasing temperatures for $T > 200$ K. As it is obvious from the relation $B_S = B_0 \times (1 + \alpha\gamma T)$, B_0 and B_S coincide at zero temperature and diverge when T increases. At room temperature, $dB_S/dT = -0.0157$ GPa/K in the HF+uCHF calculation, which agrees very well with the experimental value of Rai and Manghnani (−0.0160 GPa/K).[8]

The change of the compressibility of the crystal with p is quantitatively analyzed through B_0', B_S', and B_0'', the zero-pressure first derivatives of B_0 and B_S and the second derivative of B_0 with respect to pressure, respectively. Our HF+uCHF predictions for the first two properties at 300 K are $B_0' = 4.26$ and $B_S' = 4.15$. These numbers are reasonable, given that the actual experimental data should lie between the ultrasonic pulse−echo-overlap experiment in polycrystalline MgF_2 ($B_S' = 5.06$) of Rai and Manghnani[8] and that the ultrasonic single-crystal measurements ($B_0' = 3.85$) of Vassilou.[13] For B_0'' we find small and negative values, as observed in other ionic crystals.[35]

At this point, it is worthwhile to analyze more quantitatively the modification of the $V/V_0 - p$ curves with T. Thakur and Dwary[36] have shown that the $V/V_0 - p$ experimental data of NaCl (rocksalt phase) at 298, 500, and 800 K can be reduced almost to a single curve by plotting V/V_0 versus p/B_0. We observe in Figure 5 that our HF+uCHF EOS for MgF_2 satisfy this behavior fairly well. More specifically, for a given p/B_0 ratio, our computed V/V_0 values at $T = 0$ K and $T = 900$ K

TABLE 2: Bulk Moduli and Related Properties of the MgF_2 Rutile Phase

	B_0 (GPa)	B_S (GPa)	B_0'	B_S'	B_0'' (GPa^{-1})	dB_0/dT	dB_S/dT
static (HF)	99.06	99.06	4.25	4.25	−0.062		
static (HF+uCHF)	122.32	122.32	4.16	4.16	−0.049		
0 K (HF+uCHF)	116.93	116.93	4.13	4.13	−0.050		
300 K (HF+uCHF)	111.10	114.59	4.26	4.15	−0.055	−0.0336	−0.0157
ref 19 (HF)	103.3						
ref 16	109.7		4.38				
experimental		100.99[a]		5.06[a]			−0.0160[a]
103.4[b]							
106.2[c]							
101.7[d]			3.85[d]				

[a] Room temperature. Reference 8. [b] Room temperature. Reference 9. [c] Athermal limit. Reference 10. [d] Room temperature. Reference 13.

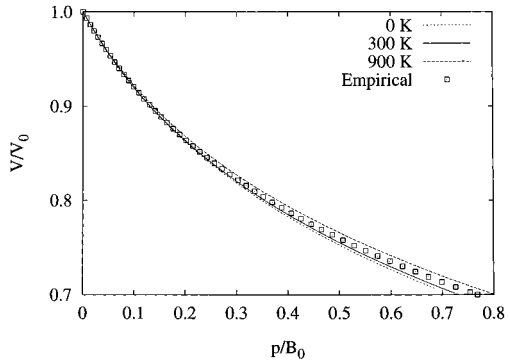

Figure 5. Reduced equation of state for the MgF_2 rutile phase. Squares stand for an empirical Vinet equation.

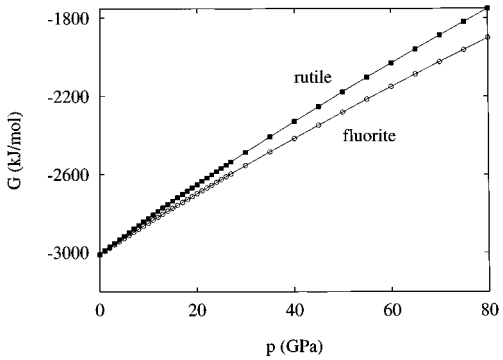

Figure 6. Phase stability diagram according to our static HF+uCHF calculations.

TABLE 3: B_0, B_0', and B_0'' Parameters for MgF_2 (Rutile) in the Static Hartree−Fock (HF, First Row) and Hartree−Fock Plus Correlation (HF+uCHF, Second Row) Calculations According to the Numerical, Vinet, and Fourth-Order Birch EOS

EOS type	B_0 (GPa)	B_0'	B_0'' (GPa^{-1})
Vinet	98.15	4.38	−0.066
	122.21	4.11	−0.047
Birch	97.44	4.78	−0.054
	121.55	4.28	−0.040
numerical	99.06	4.25	−0.062
	122.34	4.15	−0.049

differ by less than a 3%. To study this issue further, we have reduced the different sets of HF+uCHF $p - V$ data at different temperatures to the form given by the VEOS. In all cases, we have found that the VEOS is satisfied with correlation coefficients better than 0.9999 (see below), and the computed B_0' values increase very slightly with T. On the other hand, the VEOS,[34] gives a $V/V_0 - p/B_0$ curve independent of T if B_0' is T-independent. We conclude that the slight differences between all the $V/V_0 - p/B_0$ curves in our calculations are only due to the small variation of B_0' with T.

As a final remark, it is interesting to analyze the consistency of our simulation by comparing the computed EOS with the general behavior found in many real solids. We use for this purpose the *universal* Vinet EOS and the fourth-order (in energy) Birch EOS (BEOS), and find that both fit almost perfectly to our $p - V$ data. For the VEOS, the correlation coefficients are always better than 0.9999. For the BEOS, we find root mean square deviations less than 2×10^{-6} in all fittings. We stress that our $p - V$ data satisfy the empirical EOS of Vinet and Birch to a high accuracy and lead to values of B_0, B_0', and B_0'' fairly similar to those found through the numerical procedure followed in Subsection II B (see Table 3).

C. Pressure-Induced Rutile to Fluorite Phase Transition. It has been shown by Ming and Manghnani[11] that polycrystalline MgF_2 undergoes a pressure-induced phase transformation from the rutile structure to a distorted fluorite-type structure. These authors found that, below 27 GPa, only the rutile structure is present at room-T. They estimated the transition pressure (p_t) to be 30 GPa at room temperature and 19 GPa at 1573 K. In a previous X-ray experiment, Dandekar and Jamieson[5] did not report any phase transformation in this crystal up to $V/V_0 = 0.913$. From the EOS depicted in Figure 3, we expect $p \simeq 20$ GPa for that value of V/V_0. This may explain the negative result of Dandekar and Jamieson.

Our HF+uCHF results at $T = 300$ K for the rutile and fluorite structures are illustrated in Figure 6. At zero pressure, the G values of these two polymorphs are nearly coincident, both in the static and finite temperature calculations. As p increases, the fluorite structure becomes more and more stable with respect to the rutile structure. This underestimation of the stability of the rutile phase can be traced back to the current implementation of the *ai*PI method, where only spherical deformations of the ionic electron densities are allowed, and multipole−multipole electrostatic interactions are not properly accounted for.[20,21]

To obtain an insight on the effects of polarization, we have considered an approximate semiclassical model[37] in which (i) the F^- ion has a polarizability of 5.122 bohr,[3,38] (ii) the polarizability of Mg^{2+} is neglected, and (iii) the ionic wave functions are kept spherically symmetrical in the electronic structure calculation. The geometry of rutile structure was then optimized as described in section II, and its Gibbs energy at finite temperatures computed through the modified Debye model. Our results show that at $T = 300$ K and $p = 0$ GPa G decreases by 12.7 kJ/mol, giving rise to $p_t = 4$ GPa. This value is our best prediction of the thermodynamic boundary between the phases.

It is possible to obtain an upper limit for the transition from mechanical reasoning. To do so, we have computed the elastic constant $C_s = (C_{11} - C_{12})/2$ for pressures from 0 to 80 GPa. The results are plotted in Figure 7. C_s decreases with p with a

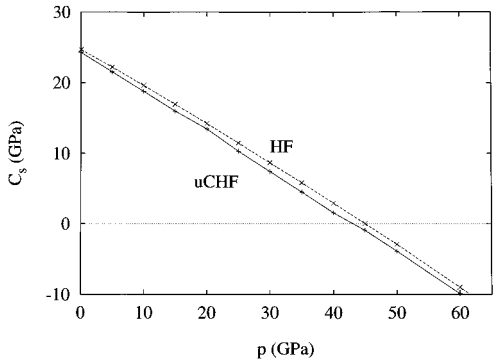

Figure 7. Pressure dependence of the shear constant for the MgF_2 rutile phase according to our HF and HF+uCHF calculations.

zero-pressure slope $C_s' = -0.48$, and C_s becomes negative at about 45 GPa. This means that, according to our calculations, the rutile structure is mechanically unstable above this pressure. At $p = 0$, we predict $C_s \simeq 24$ GPa, which is in excellent agreement with the experimental value given by Davies ($\simeq$25 GPa).[9] Striefler and Barsch[39] obtain $C_s' = -0.95$ using a rigid-ion model with effective ionic charges and only first- and second-neighbor interactions. This value is probably too negative since they predict the mechanical instability at 25 GPa, below the estimated transition pressure.[11]

It is also to be noticed that, due to the presence of hysteresis, the experimental determination of the transition pressure during loading processes gives actually an upper limit for the true thermodynamic value of p_t. Our best estimation for p_t is 4 GPa, so we predict that the experimental loading transition pressure should be above this value, as it actually is. On the other hand, based on mechanical stability considerantions, we have set an upper limit of 45 GPa for this pressure. We conclude that the thermodynamic and mechanical bounds computed in this work are compatible with the observed p_t.

D. Topological Atomic Properties. Let us now examine the topological structure of the rutile phase of MgF_2 using our *ai*PI computed electronic densities. The local symmetries of the Mg^{2+} and F^- ions are, respectively, D_{2h} and C_{2v}. This fact forces the symmetry of their topological ionic basins. We have found that the Mg^{2+} basin is a slightly distorted cube, with 2 + 4 equivalent bumped faces. Since to each face of an atomic basin there is associated a bond of the lattice, the coordination index of the cation is 6 (2 + 4). At null pressure, the Mg^{2+} bonded radii are 1.637 and 1.661 *b*, respectively. The electron density (0.0396, 0.03511 b^{-3}) and its laplacian (0.3926, 0.3508 b^{-5}) at the bond points show that the first Mg-F bond is slightly stronger than the second. The computed total ionic volume is 29.279 b^3.

The lower symmetry of the anion makes its shape harder to describe. It shows triangular coordination (1+2) with respect to the cations, with bonded radii equal to 2.037 and 2.082 bohr, respectively; and nine-fold coordination (1 + 8) with respect to the fluorides, with radii 2.3547 and 3.0858 *b*. This great separation among the different fluoride radii reflects the larger deformability of the anion.

At first sight, the existence of anion−anion bonds may sound a little perturbing, but it is a topological requirement that was found to be important for understanding the stability of the lattices.[24] In our case it also appears that the larger bond is the weaker and has larger coordination index. The fluoride volume turns out to be 89.404 b^3, approximately three times the cationic volume. It sould be stressed, however, that a bond in Bader's sense is a new objective concept, and that its relation to chemical bonding theory has still to be worked out in detail, at least in those cases where classical bond analogues are lacking.

Figure 8. Ionic basins for the rutile phase of MgF_2 at zero pressure. A complete fluoride (center) coordination shell is shown, except four frontal anions that have been excluded to improve the vision of the cations.

We found an anion basin with 12 faces. Figure 8 shows the atomic basins of the coordination shell around a central fluoride. The four frontal coordinating anions have been clipped out from the figure to allow a clearer view of the cations. Several important facts appear from a closer examination of the picture. First, notice that the homeomorphism between atomic basins and polyhedra is not only of a mathematical nature. The basins are *actually* recognizable as polyhedra. Second, the basins fill completely the space. The stringent requirements posed by topology on the number and types of critical points in the lattice force the quasi-bidimensional wings shown by the cations. These wings avoid a forbidden anion-anion contact at several places and, therefore, the formation of more anion faces. The 2 + 4 coordination for the cation and the 1 + 2, 1 + 8 coordination for the anion are easily recognized. Finally, it is interesting to observe how the bumps of the cation faces correspond to depressions in the anion faces, reinforcing the association of hardness for cations and deformability for anions.

Regarding atomic properties, we will only comment on results for the integration of the charge density over the basins. At null pressure, the charge found for the fluoride is −0.942 |e|. This result reveals a very ionic crystal structure. Pressure induces a reduction of the lattice parameter and a rather important reorganization of the electronic density. The effects of these changes on the topology of the density and bonding properties are not straightforward and have not been reported previously. We have not found, up to now, any crystalline phase whose electronic topological structure changes as the lattice parameters shrink. MgF_2 is not an exception and keeps the same general pattern described above. Figure 9 shows the evolution of the different radii with the *a* lattice parameter. All of them show a practically perfect linear relation with *a* and rather similar slopes. This surprising linear behavior admits a very simple rationalization. It is easy to show that, if the density along a bond line is mainly the sum of exponentially decreasing functions located at the two bonded nuclei, the position of the bond critical point is a linear function of the internuclear separation. This is certainly the case in many ionic materials.

It is interesting to observe that the difference in the radii of the two different Mg−F bonds increases with pressure, the stronger bond displaying a slightly greater variation than the weaker one. This result can be understood as a consequence of the different deformability of the two ionic species. Such difference is clearly illustrated by the pressure dependence of the ratio of topological ionic volumes, $r = v(F^-)/v(Mg^{2+})$. We find that *r* is also linear with *a* and decreases from 3.053 at null pressure to 2.622 at 100 GPa, revealing that the anion compression is much easier. Anions changes its volume by a factor 1.50 on compression, cations by a factor 1.29.

The topological charges vary also linearly with pressure. The fluoride charge decreases, in absolute value, from −0.942 |e|

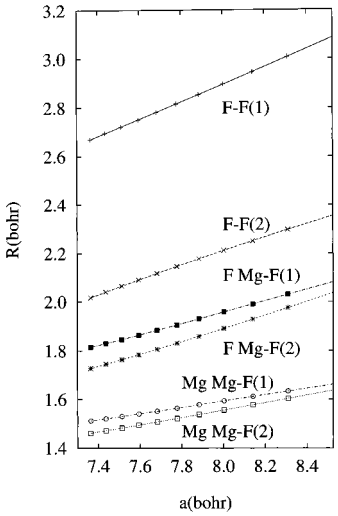

Figure 9. Variation of the topological bond radii of the rutile phase of MgF_2 with the lattice parameter *a*. When several bonds of the same type are present, they are distinguished by a numeral.

at null pressure to −0.913 |e| at 100 GPa. Thus, Bader's ionicity of this crystal decreases very slowly with pressure, in agreement with qualitative expectations, based on classical ideas. We must also notice that the relation between Bader's ionicity or covalency and orbital mixing should be further investigated.

IV. Conclusions

We have investigated the structural and thermodynamic properties of the MgF_2 crystal in wide ranges of pressure and temperature using the quantum-mechanical ab initio perturbed ion method. Vibrational contributions on these properties have been included by means of a quasi-harmonic Debye model. The theory of Bader[22] has been adopted to analyze the topology of the electron density of this system.

Our results for the static properties at zero pressure are in rather good agreement with the experiment when correlation energy corrections are included in the calculation. The quasi-harmonic Debye model accounts successfully for the change with *T* of the thermodynamic properties studied here. The E_{latt} versus *V* curve given by the ab initio perturbed ion model yields EOS in agreement with the general behavior found in real solids. Our results are consistent with measured elastic moduli. According to criteria of thermodynamic and mechanical stability, we confine the rutile to fluorite transition pressure in the loading process to the range 4−45 GPa. Experiments at room and high temperature give values for this property within this theoretical range. The exploration of this issue suggests, however, the need of a generalization of the *ai*PI methodology to allow for nonspherical distortions of the ionic electron densities. This improvement will probably increase the lower boundary for p_t.

The bonding picture emerging from the topological study is coherent with classical thinking: small, nonpolarizable cations surrounded by larger polarizable anions. An interesting fact, already found in other systems,[23] is the existence of anion−anion bonds, whose importance in the overall stabilization of the lattice needs to be studied. We have also performed the integration of several properties over the different ionic basins, yielding ionic charges and volumes that classify MgF_2 as a highly ionic compound, the degree of ionicity decreasing with increasing pressure.

Acknowledgment. The authors want to express their gratitude to Professor L. Pueyo for the careful reading of the manuscript. We are grateful to the Centro de Cálculo Científico, Universidad de Oviedo, for the CONVEX facility. Financial support from the Spanish Dirección General de Investigación Científica y Tecnológica (DGICYT), Project PB96-0559, is also acknowledged. One of us (M.A.B.) is indebted to the Spanish Ministerio de Investigación y Ciencia for a postgraduate grant.

References and Notes

(1) Todd, S. S. *J. Am. Chem. Soc.* **1949**, *71*, 4115.
(2) Baur, V. W. H. *Acta Crystallogr.* **1956**, *9*, 515.
(3) Rao, K. V. K.; Naiudu, S. V. N.; Setty, P. L. N. *Acta Crystallogr.* **1962**, *15*, 528.
(4) Cutler, H. R.; Gibson, J. J.; McCarthy, K. A. *Solid State Commun.* **1968**, *6*, 431.
(5) Dandekar, D. P.; Jamieson, J. C. *Trans. Am. Crystallogr. Assoc.* **1968**, *5*, 19.
(6) Jones, L. E. A.; Liebermann, R. C. *Phys. Earth Planet. Inter.* **1974**, *9*, 101.
(7) Baur, W. H. *Acta Crystallogr.* **1976**, *32*, 2200.
(8) Rai, C. S.; Manghnani, M. H. *J. Am. Ceram. Soc.* **1976**, *59*, 499.
(9) Davies, G. *Earth Planet. Sci. Lett.* **1977**, *34*, 300.
(10) Jones, L. E. A. *Phys. Chem. Miner.* **1977**, *1*, 179.
(11) Ming, L.; Manghnani, M. H. *Geophys. Res. Lett.* **1979**, *6*, 13.
(12) Vidal-Valat, G.; Vidal, J. P.; Zeyen, C. M. E.; Kurki-Suonio, K. *Acta Crystallogr. B* **1979**, *35*, 1584.
(13) Vassiliou, J. K. *J. Appl. Phys.* **1985**, *57*, 4543.
(14) Kim, Y. S.; Gordon, R. G. *Phys. Rev. B* **1974**, *9*, 3548.
(15) Muhlhausen, C.; Gordon, R. G. *Phys. Rev. B* **1981**, *23*, 900.
(16) Kim, H. J.; Choo, W. K. *Int. J. Mod. Phys. B* **1994**, *8*, 1543.
(17) Allan, N. L.; Hines, R. I.; Towler, M. D.; Macdrodt, W. C. *J. Chem. Phys.* **1994**, *100*, 4710.
(18) Nga, Y. A.; Ong, C. K. *J. Chem. Phys.* **1993**, *98*, 3240.
(19) Catti, M.; Pavesse, A.; Dovesi, R.; Roetti, C.; Causa, M. *Phys. Rev. B* **1991**, *44*, 3509.
(20) Luaña, V.; Pueyo, L. *Phys. Rev. B* **1990**, *41*, 3800.
(21) Luaña, V.; Martín Pendás, A.; Recio, J. M.; Francisco, E.; Bermejo, M. *Comput. Phys. Commun.* **1993**, *77*, 107.
(22) Bader, R. F. W. *Atoms in Molecules*; Oxford University Press: Oxford, 1990.
(23) Pendás, A. M.; Castro, A. C.; Luaña, V. *Phys. Rev. B* **1997**, *55*, 4275.
(24) Luaña, V.; Castro, A. C.; Pendás, A. M. *Phys. Rev. B* **1997**, *55*, 4285.
(25) Martín Pendás, A.; Recio, J. M.; Flórez, M.; Luaña, V.; Bermejo, M. *Phys. Rev. B* **1994**, *49*, 5858.
(26) Clementi, E.; Roetti, C. *At. Data Nucl. Data Tables* **1974**, *14*, 177.
(27) Chakravorty, S. J.; Clementi, E. *Phys. Rev. A* **1989**, *39*, 2290.
(28) Press, W. H.; Flannery, B. P.; Teukolski, S. A.; Vetterling, W. T. *Numerical Recipes*; Cambridge University Press: Cambridge, 1986.
(29) Robie, R. A.; Edwards, J. L. *J. Chem. Phys.* **1966**, *37*, 2659.
(30) Poirier, J. P. *Introduction to the Physics of the Earth's Interior*; Cambridge University Press: New York, 1991.
(31) Kandill, H.; Greiner, J.; Ayers, A.; Smith, J. *J. Appl. Phys.* **1981**, *52*, 759.
(32) Blanco, M. A.; Pendás, A. M.; Francisco, E.; Recio, J. M.; Franco, R. *J. Mol. Struct. (THEOCHEM)* **1996**, *368*, 245.
(33) Lide, D. R., Ed. *Handbook of Chemistry and Physics*; Chemical Rubber Company: Boca Raton, FL, 1991.
(34) Vinet, P.; Rose, J. H.; Ferrante, J.; Smith, J. R. *J. Phys.: Condens. Matter* **1989**, *1*, 1941.
(35) Hart, S.; Greenwood, P. H. *Solid State Commun.* **1983**, *46*, 161.
(36) Thakur, K. P.; Dwary, B. D. *J. Phys. C* **1986**, *19*, 3069.
(37) Blanco, M. A.; Ph.D. thesis, Universidad de Oviedo, Spain, 1997.
(38) Tessman, J. R.; Kahn, A. H.; Shockley, W. *Phys. Rev. B* **1953**, *92*, 890.
(39) Striefler, M.; Barsch, G. R. *Phys. Status Solidi B* **1974**, *64*, 613.